Carbohydrate Polymers 92 (2013) 1078–1085

Contents lists available at SciVerse ScienceDirect

Carbohydrate Polymers

journal homepage: www.elsevier.com/locate/carbpol

Preparation and antimicrobial property of chitosan oligosaccharide derivative/rectorite nanocomposite

Bo Liu [a], Xiaoying Wang [a,*], Chunsheng Pang [a], Jiwen Luo [b], Yuqiong Luo [a], Runcang Sun [a,c,**]

[a] State Key Laboratory of Pulp & Paper Engineering, South China University of Technology, Guangzhou 510640, Guangdong, China
[b] Key Laboratory of Theoretical Chemistry of Environment, Ministry of Education, School of Chemistry and Environment, South China Normal University, Guangzhou 510006, China
[c] Institute of Biomass Chemistry and Technology, Beijing Forestry University, Beijing 100083, China

ARTICLE INFO

Article history:
Received 27 August 2012
Received in revised form 21 October 2012
Accepted 22 October 2012
Available online 30 October 2012

Keywords:
Quaternized carboxymethyl chitosan oligosaccharide
Rectorite
Nanocomposite
Thermal stability
Antimicrobial activity

ABSTRACT

Microwave irradiation was used to intercalate quaternized carboxymethyl chitosan oligosaccharide (QCMCO) into the layer of rectorite (REC) to prepare QCMCO/REC (QCOR) nanocomposites in 70 min, which was much faster than conventional heating method of 48 h. The structures and morphology of QCOR nanocomposites were characterized by XRD, TEM, FT-IR and zeta potential analysis, the thermal behavior and antimicrobial activity of QCOR nanocomposites were also discussed. The results revealed that the interlayer distance of QCOR nanocomposites enlarged with the increase of QCMCO content, hydrogen bonding and electrostatic interaction between QCMCO and REC took place. As compared to QCMCO, the crystallinity of QCOR nanocomposites reduced, the thermal stability of QCOR nanocomposites improved, and the inhibitory activity of QCOR nanocomposites against microorganisms was stronger, the lowest minimum inhibition concentration was only 0.025% (w/v), the antimicrobial mechanism was discussed via TEM and SEM micrographs.

1. Introduction

Chitosan is composed of β-(1,4)-2-amino-2-deoxy-D-glucose (GlcN) and β-(1,4)-2-acetamido-2-deoxy-D-glucose (GlcNAc) binary linear copolymer (Kong, Chen, Xing, & Park, 2010; Q. Wang, Zhang, Hu, Yang, & Du, 2008). As a broad-spectrum antibacterial agent, it can inhibit the growth of several bacteria and fungi (Kong et al., 2010; Vinsova & Vavrikova, 2011; Xia, Liu, Zhang, & Chen, 2011). Quaternized carboxymethyl chitosan (QCMC) is the water-soluble amphoteric derivative of chitosan (Liu, Wang, Li, et al., 2012; Liu, Wang, Yang, Sun, 2012; Sun, Du, Fan, Chen, & Yang, 2006). Many researchers have reported the superior antibacterial properties of high-molecular-weight QCMC (Aranaz, Harris, & Heras, 2010; Sun et al., 2006; Vinsova & Vavrikova, 2011), but there are very few reports about the antimicrobial activity of low-molecular-weight QCMC (below 20,000 Da). Since chitosan and its derivatives with low molecular weight have better biological activity (Dutta, Tripathi, & Dutta, 2012), the study on the antibacterial properties of low-molecular-weight quaternized carboxymethyl chitosan oligosaccharide (QCMCO) is of great significance for its further biological application.

In addition, rectorite (REC) is a 2:1 typed layered silicate, the previous study demonstrates that it has not antibacterial activity by itself (Zhou et al., 2010), but it shows dual performance of adsorbing bacteria and killing bacteria when the cationic material with antibacterial activity was intercalated into the interlayer of REC (Deng et al., 2012; Q. Wang, Zhang, Hu, Yang, & Du, 2007; X. Wang, Du, Luo, Lin, & Kennedy, 2007; X. Wang et al., 2009, 2006; X.Y. Wang, Du, Sun, & Lin, 2009; X.Y. Wang et al., 2012). But there has no report about inserting QCMCO into the interlayer of REC in order to combine both antibacterial advantages.

Chitosan-based layered silicate nanocomposite draw people's attention for coupling of numerous merits of chitosan and layered silicate (Deng et al., 2012; Liu, Wang, Yang, & Sun, 2011; Liu, Wang, Yang, Wang, & Sun, 2011; X. Wang et al., 2009, 2006; X.Y. Wang et al., 2009), but at present, its preparation mostly adopt solution intercalation technique under traditional heating condition, the reaction time is 6–48 h, and the reproducibility is poor (Liu, Wang, Yang, & Sun, 2011; Liu, Wang, Yang, Wang, et al., 2011; X. Wang et al., 2009; X.Y. Wang et al., 2009). Microwave radiation method, invented by Gerda in 1986 (Gedye, Smith, & Westaway, 1986), is attracting more and more attention for its fast, simple and efficient advantages. Many scholars prepared various chitosan derivatives and low-molecular-weight chitosan by microwave irradiation method (Liu, Wang, Li, et al., 2012; Liu,

* Corresponding author. Tel.: +86 20 87111861; fax: +86 20 87111861.
** Corresponding author at: State Key Laboratory of Pulp & Paper Engineering, South China University of Technology, Guangzhou 510640, Guangdong, China. Tel.: +86 20 87111861; fax: +86 20 87111861.
E-mail addresses: xyw@scut.edu.cn (X. Wang), rcsun3@bjfu.edu.cn (R. Sun).

0144-8617/$ – see front matter © 2012 Elsevier Ltd. All rights reserved.
http://dx.doi.org/10.1016/j.carbpol.2012.10.060

Wang, Yang, et al., 2012; Luo, Wang, Xia, & Wu, 2010; Mecwan, Rapalo, Mishra, Haggard, & Bumgardner, 2011; Tishchenko et al., 2011), Kabiri and other researchers prepared chitosan-based montmorillonite nanocomposite within several minutes (El-Sherif & El-Masry, 2011; Kabiri, Mirzadeh, & Zohuriaan-Mehr, 2007) using microwave irradiation. But so far, there are few reports about chitosan-based REC nanocomposite prepared by microwave irradiation method (Liu, Wang, Li, et al., 2012; Liu, Wang, Yang, et al., 2012; Liu, Wang, Yang, & Sun, 2011; Liu, Wang, Yang, Wang, et al., 2011).

In this paper, QCMCO/REC (QCOR) nanocomposite was prepared rapidly under microwave radiation, their structures were characterized by XRD, TEM, FT-IR, zeta potential analysis and TGA techniques. Moreover, the inhibition ability of QCOR nanocomposites against four bacteria and one fungus was evaluated, and the antibacterial mechanism was discussed.

2. Experimental

2.1. Materials

Chitosan (CS) was purchased from Yuhuan Ocean Biochemical Co. (Zhejiang, China). The degree of deacetylation was 82%, its weight average molecular weight (*Mw*) was 1.5×10^4, 2,3-epoxypropyltrimethyl ammoniumchloride (ETA) was purchased from Dongying Guofeng Fine Chemical Co. Ltd. (Shandong, China), calcium rectorite (Ca^{2+}-REC) with a cation exchange capacity (CEC) value of 45 mmol/100 g refined from the clay minerals was provided by Hubei Mingliu Inc. Co. (Wuhan, China). All other chemicals were of analytical grade.

2.2. Preparation of QCMCO

Quaternized carboxymethyl chitosan oligosaccharide (QCMCO) was prepared by grafting carboxymethyl groups and quaternary ammonium groups on chitosan chain under microwave irradiation according to the previous study (Liu, Wang, Li, et al., 2012; Liu, Wang, Yang, et al., 2012). Briefly, the carboxylmethylation of chitosan was performed by using chloroacetic acid as modification agent at 800 W and 70 °C for 25 min, and then the carboxylmethyl chitosan was quaternized at 800 W and 75 °C for 70 min. The molar ratio of chloroacetic acid and ETA to amino groups of chitosan was 4:1 and 6:1, respectively. The reaction mixture was precipitated by acetone and then washed to neutral pH value. Finally, QCMCO was obtained by dialysis against distilled water and then lyophilization at −50 °C. The *Mw* of the prepared QCMCO was 1.85×10^4 which was determined by gel permeation chromatography method. The degree of substitution of carboxymethyl groups and quaternary ammonium groups were 0.88 and 0.75, respectively, which was determined by deposit-titration method.

2.3. Preparation of QCOR nanocomposites

Quaternized carboxymethyl chitosan oligosaccharide/rectorite (QCOR) nanocomposites were prepared via the intercalation of QCMCO into REC. 0.1 g of REC was dispersed in distilled water, the resulting clay suspension was left for 24 h after vigorous stirring for 30 min and then put into the microwave system. QCMCO solution was obtained in distilled water and dropped slowly into REC suspension and reacted under microwave irradiation for 70 min at 600 W and 80 °C. Finally, QCOR nanocomposites were obtained after being freeze-dried at −40 °C. The nanocomposites with weight ratios of QCMCO to REC of 2:1, 4:1, 8:1 and 20:1 were recorded as QCOR-1, QCOR-2, QCOR-3 and QCOR-4, respectively.

2.4. Characterization of QCOR nanocomposites

X-ray diffraction (XRD) patterns of powder sample were obtained using D8 advance X-ray diffractometer (Bruker, Germany) with a Cu *Kα* radiation (λ = 0.15418 nm) at 40 kV and 50 mA at 25 °C. The relative intensity was recorded in the scattering range of 1–10° at a scanning speed of 1°/min.

The microstructure of REC and QCOR nanocomposite were taken using a JEM-2010 HR transmittance electron microscope (TEM) (JEOL, Japan) at an accelerating voltage of 200 kV. Clay sample for TEM studies was dispersed in 50% ethanol solution and dropped on Cu mesh grids, then dried in an oven at 50 °C for 10 min. Ultrathin films of QCOR nanocomposite were prepared by cutting from the epoxy block with the embedded nanocomposite sheet using an UCL/FC6 ultratome (LEICA, Australia).

Fourier transform infrared (FT-IR) spectra were performed on a Nicolet FT-IR 5700 spectrophotometer (Bruker, Germany) at room temperature by the KBr pellets method. The spectra were collected for each measurement over the spectral range 4000–400 cm^{-1} with a resolution of 4 cm^{-1}.

2.5. Crystallization behavior of QCOR nanocomposites

Crystallization behavior was determined by the X-ray diffraction (XRD), the experiment was performed using a diffractometer type D8 advance (Bruker, Germany) with Cu target and *Kα* radiation (λ = 0.15418 nm) at 40 kV and 50 mA. The scanning rate was 2°/min and the scanning scope was 5–45°.

2.6. Zeta potential of QCOR nanocomposites

Zeta potential was determined by 3000HSA typed nanometer particle size and potential analyzer (Malven, England), sample concentration was 0.1% (w/v).

2.7. Thermal stability of QCOR nanocomposites

Thermogravimetric analysis (TGA) was carried out on a SDT-Q500 simultaneous thermal analyzer (TA, USA) under a nitrogen atmosphere from room temperature to 600 °C and at a heating rate of 10 °C/min.

2.8. Antibacterial assay

Gram-positive bacteria *Staphylococcus aureus*, *Bacillus subtilis*, Gram-negative bacteria *Escherichia coli*, *Pseudomonas aeruginosa* and Fungus *Aspergillus niveus* were provided by Guangdong Institute of Microbiology and incubated on nutrient agar (peptone 1%, beef extract 0.5%, NaCl 0.5%, agar 2%, pH = 7.2).

2.8.1. Determination of the minimum inhibition concentration (MIC)

The minimum inhibition concentration (MIC) was defined as the lowest concentration required inhibiting the growth of bacteria, i.e. the concentration at which no microorganism colony or less than 5 colonies were visible.

The microorganism suspension was adjusted by sterile distilled water to 10^5–10^6 cell/ml. The QCOR nanocomposites, QCMCO and REC suspensions were prepared in PBS. The resulting solutions and the nutrient agar were autoclaved at 121 °C for 20 min. 1 mL of each sample were added to sterile petri-dishes together with 9 mL nutrient agar. A loop of each microorganism suspension was inoculated on cooled nutrient medium by means of drawing a stripe. The microorganisms were cultured at 37 °C. MICs values were read after a 24 h of culture.

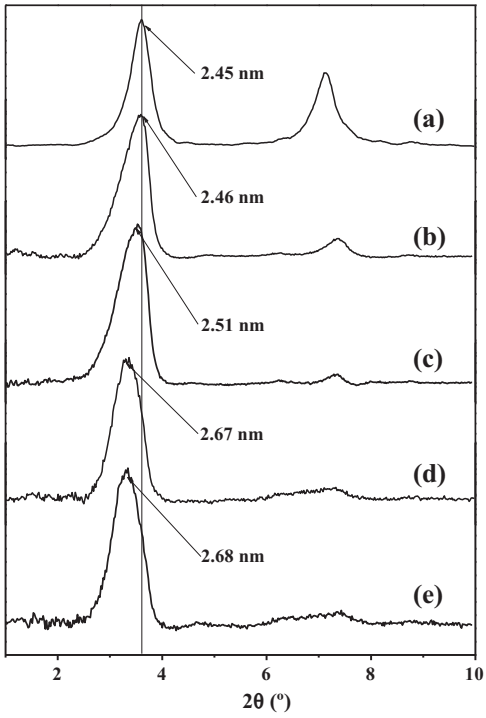

Fig. 1. XRD patterns of REC and QCOR nanocomposites: (a) REC; (b) QCOR-1; (c) QCOR-2; (d) QCOR-3 and (e) QCOR-4.

2.8.2. Observation by scanning electron microscope

1 mL microorganism suspension was centrifuged at 11,000 rpm for 10 min, the supernatant was removed, the resulting pellets were resuspended in 1 mL 0.1 M PBS and QCOR nanocomposite, incubated at 37 °C for 20 min and then centrifuged to remove the supernatant. The resulting pellets were washed twice with 0.1 M pH 7.2 PBS, pre-fixed with 2.5% glutaraldehyde in 0.1 M pH 7.2 PBS, and then re-fixed with 4% glutaraldehyde in the same PBS for 2 h at room temperature and washed once with the same PBS. The pellets was dehydrated in a graded series of acetone, vacuum dried and sprayed, then observed by S-3700N scanning electron microscope (SEM) (Hitachi, Japan).

2.8.3. Observation by transmission electron microscope

1 mL microorganism suspension was centrifuged at 11,000 rpm for 10 min and removed the supernatant, the resulting pellets were resuspended in 1 mL 0.5% PBS and QCOR nanocomposite, incubated at 37 °C for 20 min and then centrifuged to remove the supernatant. The resulting pellets were washed twice with 0.1 M pH 7.2 phosphate buffer (PBS) and pre-fixed with 2.5% glutaraldehyde in 0.1 M pH 7.2 PBS. Then they were re-fixed with OsO4 in 0.1 M pH 7.2 PBS for 2 h at room temperature, washed the bacterial cells once with the same PBS and dehydrated in a graded series of ethanol, washing with acetone and embedding in Spur low-viscosity medium. Thin sections of the specimens were cut with a diamond knife on an UCL/FC6 ultratome (LEICA, Australia) and the sections were double-stained with saturated uranyl acetate and lead citrate. The grids were examined with an JEM-2010 HR transmittance electron microscope (TEM) (JEOL, Japan) at an accelerating voltage of 200 kV.

3. Results and discussion

3.1. Structure and morphology of QCOR nanocomposites

XRD patterns of REC and QCOR nanocomposites are shown in Fig. 1. As compared to REC, the d_{001} diffraction peak of QCOR nanocomposites shifts toward lower angle, which indicates that QCMCO entered into the interlayer of REC (X.Y. Wang et al., 2012). It is noted that the interlayer distance of QCOR nanocomposites is lower than that of QCMCO/OREC nanocomposites (data did not show here), the possible reason is as follows: OREC is hydrophobic layered silicate, which is preferable for the entrance of polymer, on the contrary, natural REC is hydrophilic (De Paiva, Morales, & Valenzuela Diaz, 2008; Liu, Wang, Yang, & Sun, 2011; Liu, Wang, Yang, Wang, et al., 2011); moreover, the original interlayer distance of OREC is 2.94 nm, which is larger than 2.45 nm of REC, this larger interlayer spacing of OREC provides more room for the intercalation of QCMCO. In addition, previous reports investigated that in the same condition we can get exfoliated QCMC/REC nanocomposite (Liu, Wang, Li, et al., 2012; Liu, Wang, Yang, et al., 2012), in that case, *Mw* of QCMC was 8.28×10^4, which is higher than that of QCMCO in this work, it implies that QCMC with high *Mw* can provide more driving force to enter the interlayer of REC. What's more, Fig. 1 shows that the interlayer distance of the QCOR nanocomposites enlarged as the QCMCO amount increased, but when the mass ratio of QCMCO to REC further increased to be 8:1, the interlayer distance of REC did not increase markedly, the fact reveals that more QCMCO can also induce the better intercalation, because in this case, larger driving force for intercalation can be obtained (Q. Wang, Hu, Du, & Kennedy, 2010; X.Y. Wang et al., 2010).

From the above results, the conclusion can be drawn that during the intercalation reaction between layered silicate and polymer, the change of the interlayer distance of clay is closely related to its surface characteristics, the molecular weight and the content of polymer.

Fig. 2 exhibits the TEM micrographs of QCOR-4 nanocomposite, in the figure, the dark lines represent the silicate layer of REC while the bright area represent the QCMCO matrix. Compared to REC, the enlarged layers can be seen in the TEM micrograph of QCOR-4 nanocomposite. Moreover, in the low magnification image (Fig. 2c), it can be seen that REC are dispersed uniformly in QCMCO matrix, while in the high magnification image (Fig. 2d), QCMCO have entered into the interlayer of REC, and classical rectorite layered structure occurs in the QCOR nanocomposite, which is an indicative of intercalated chitosan-based layer silicate nanocomposite. The interlayer distance was measured to be about 2.67 nm, which agrees with the XRD analysis.

3.2. Interaction between REC and QCMCO

Fig. 3 shows FT-IR spectra of REC, QCMCO and QCOR nanocomposites, it can be seen from the figure that with the increase of QCMCO content, O—H peaks of REC at 3638 cm^{-1} were weaker and weaker until disappeared, and obviously have no correlation with the content of REC. Moreover, in the spectrum of QCMCO, the characteristic peaks at 1480 cm^{-1} was belonged to the vibration of quaternary ammonium groups, and the peaks at 1601 cm^{-1} and 1406 cm^{-1} were ascribed to the vibration of —COO groups (Q. Wang et al., 2007, 2010; X. Wang et al., 2007; X.Y. Wang et al., 2010), they are weaker and weaker in the spectra of QCOR nanocomposites, and have no relation with the amount of QCMCO; more notably, in contrast with the spectrum of QCMCO, the N—H bonded to O—H peak at 3417 cm^{-1} and the —COO peaks at 1601 cm^{-1} and 1406 cm^{-1} in the spectra of QCOR nanocomposites shifted toward lower frequency. All above results indicate that there were hydrogen bonding and electrostatic interaction between QCMCO and REC (Liu, Wang, Yang, et al., 2012; Liu, Wang, Li, et al., 2012; X. Wang et al., 2006).

Table 1 gives the zeta potential values of REC, QCMCO and QCOR nanocomposites. From the table, it can find that REC itself has a negative charge, its zeta potential value is −33.8 mV, the zeta potential value of QCMCO is +35.5 mV, while the QCOR nanocomposites have

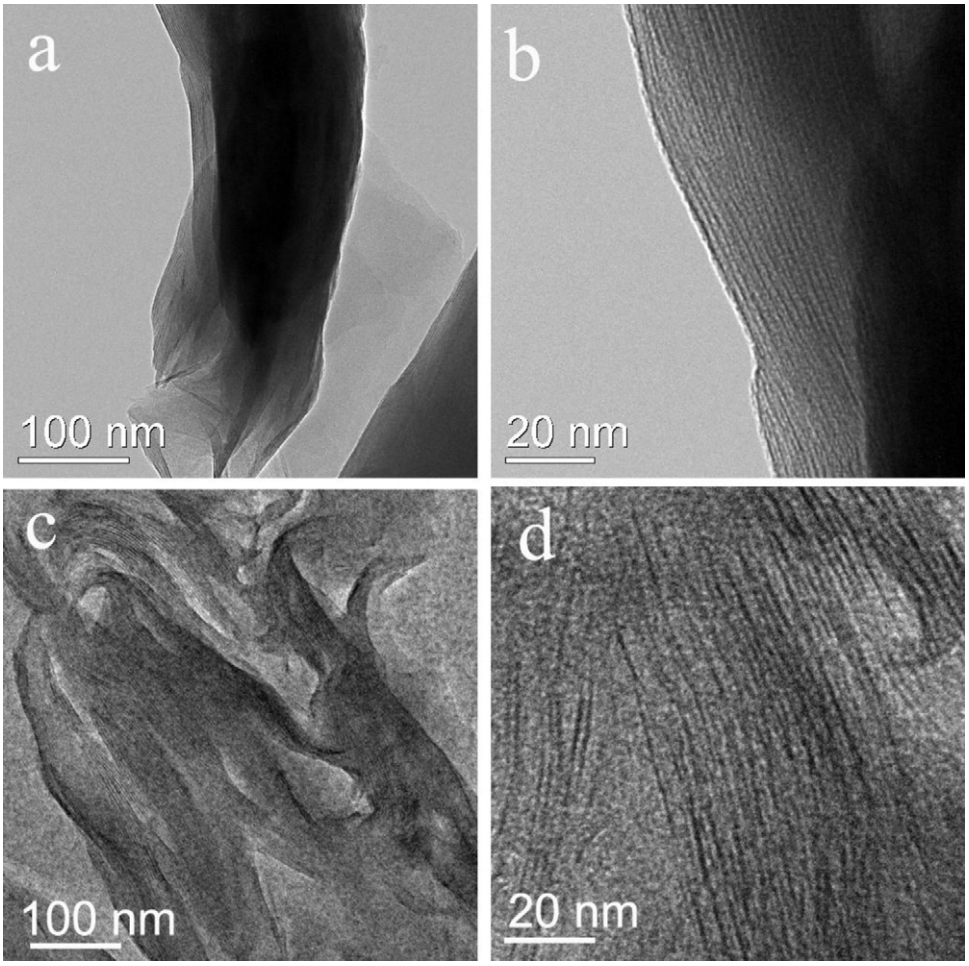

Fig. 2. TEM micrographs of (a, b) REC and (c, d) QCOR-4 nanocomposite.

positive surface charge, and their potential are closely related with the QCMCO content. With the increase of QCMCO content (QOOR-1 to QOM-4), the surface charge value of QCOR nanocomposites increased from +4.6 mV to +29.5 mV. It is noted that the potential value of QCOR nanocomposites was not the simple addition of the value of QCMCO and REC, revealing the strong electrostatic interaction between QCMCO and REC (X. Wang et al., 2009; X.Y. Wang et al., 2009), which is in accordance with the FT-IR results.

The XRD patterns from 5° to 45° of REC, QCMCO and QCOR nanocomposites are presented in Fig. 4. It can be seen from the figure that there are several obvious peaks of pure REC, the peaks at 7.3°, 18°, 20°, 27.4°, 28.9° and 35.3° are corresponded to the crystallinity of (0 0 2), (0 0 5), (1 1 1), (0 0 7), (0 0 8) and (1 3 0) crystal planes, respectively, while QCMCO has only one wide peak at $2\theta = 21.1°$. Compared with QCMCO and REC, the corresponding diffraction heights in the XRD patterns of the QCOR nanocomposites are lower, especially the peak heights in (1 1 1), (0 0 8) and (1 1 3) crystal planes, which have no relationship with REC's content, it reveals that the interaction between QCMCO and REC happened in the intercalation process (Ojijo, Malwela, Ray, & Sadiku, 2012; X. Wang et al., 2009; X.Y. Wang et al., 2009). Careful observation indicates that the (0 0 5) crystallinity peak of REC in QCOR nanocomposite shifts toward high angle, and there are new crystallization peaks at 11.7° and 29.6°, these results

Table 1
Zeta potential (mV, $n = 3$) and MICs (%, w/v, $n = 3$) of REC, QCMCO and QCOR nanocomposites.

Samples	Zeta potential	Gram-negative bacteria		Gram-positive bacteria		Fungus
		Escherichia coli	*Pseudomonas aeruginosa*	*Bacillus subtilis*	*Staphyloccocus aureus*	*Aspergillus niger*
Blank		–[a]	–	–	–	–
PBS		–	–	–	–	–
REC	−33.8 ± 0.4	–	–	–	–	–
QCOR-1	+4.6 ± 0.1	1	1	0.1	0.05	–
QCOR-2	+22.5 ± 0.4	1	1	0.1	0.05	–
QCOR-3	+24.2 ± 0.4	0.5	1	0.05	0.025	–
QCOR-4	+29.5 ± 0.8	0.5	0.5	0.05	0.025	1
QCMCO	+35.5 ± 1.9	1	1	0.1	0.05	2

[a] No antibacterial property.

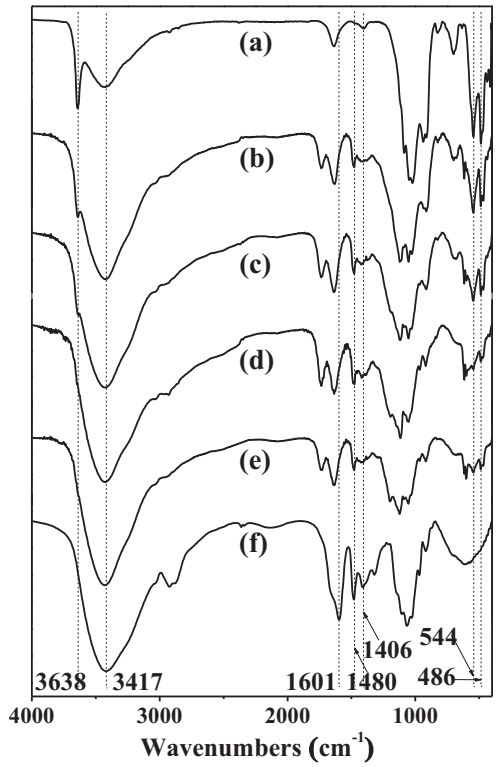

Fig. 3. FT-IR spectra of REC, QCMCO and QCOR nanocomposites: (a) REC; (b) QCOR-1; (c) QCOR-2; (d) QCOR-3; (e) QCOR-4 and (f) QCMCO.

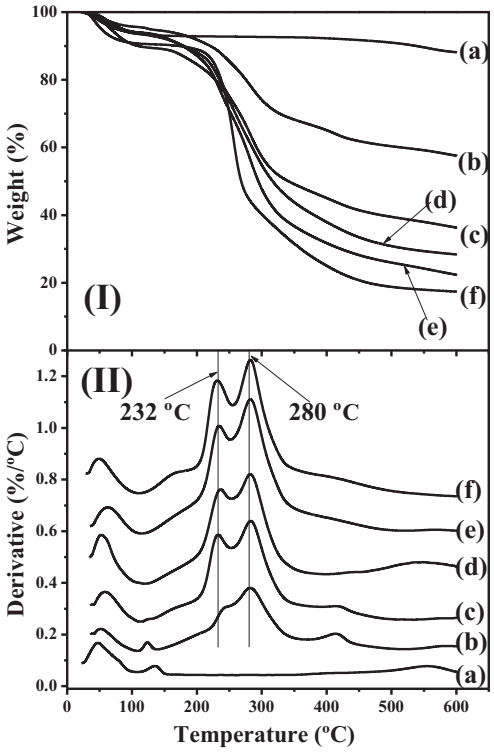

Fig. 5. TGA and DTG curves of REC, OCMCO and QCOR nanocomposites: (a) REC; (b) QCOR-1; (c) QCOR-2; (d) QCOR-3; (e) QCOR-4 and (f) QCMCO.

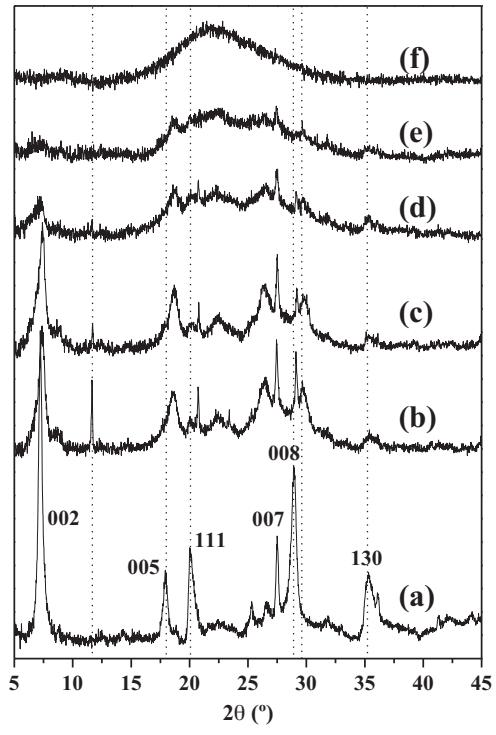

Fig. 4. XRD patterns of REC, QCMCO and QCOR nanocomposites: (a) REC; (b) QCOR-1; (c) QCOR-2; (d) QCOR-3; (e) QCOR-4 and (f) QCMCO.

further demonstrate that there were strong interaction between QCMCO and REC, which coincides with the FT-IR and zeta potential results.

3.3. Thermal stability of QCOR nanocomposites

Fig. 5 shows the TGA and DTG curves of REC, OCMCO and QCOR nanocomposites. It can observe that REC has not obvious degradation process at 200–600 °C, so the degradation of QCOR nanocomposites in this phase was mainly caused by the degradation of QCMCO. The two decomposition stages of QCOR nanocomposites were due to thermal dehydration and the degradation of QCMCO molecular chains itself, which agrees with the previous reports about chitosan-based layered silicate nanocomposites (X. Wang et al., 2009, 2006; X.Y. Wang et al., 2009).

As shown in Fig. 5I, the residual weight of QCOR-1 to QCOR-4 nanocomposites were 57%, 36%, 28% and 24% at 600 °C, respectively, which were higher than that of QCMCO (18%), and they were not proportional to the content of REC since REC contents of QCOR-1 to QCOR-4 nanocomposites were 33.3%, 20%, 11.1% and 4.8%, respectively. The result indicates that the thermal stability of QCMCO improved after the incorporation of REC. It can be explained that the continuous decomposition of QCMCO was restricted because of the limited layer space of REC and the strong interaction between QCMCO and REC; higher heat-resistant capacity of mica in REC was another important cause (Cheng et al., 2012; Karim et al., 2009).

As can be seen from Fig. 5II, the T_{max} (the temperature when the rate of degradation reaches a maximum) of QCOR nanocomposites did not increase obviously with the import of REC compared with the previous reports (X. Wang et al., 2006), this may be due to the smaller Δd_{001} (the increased interlayer distance after the intercalation) of QCOR nanocomposites, which can limit the entrance of QCMCO molecules into REC space, and thereby it is insufficient enough for REC to provide more protection for QCMCO (X. Wang et al., 2006).

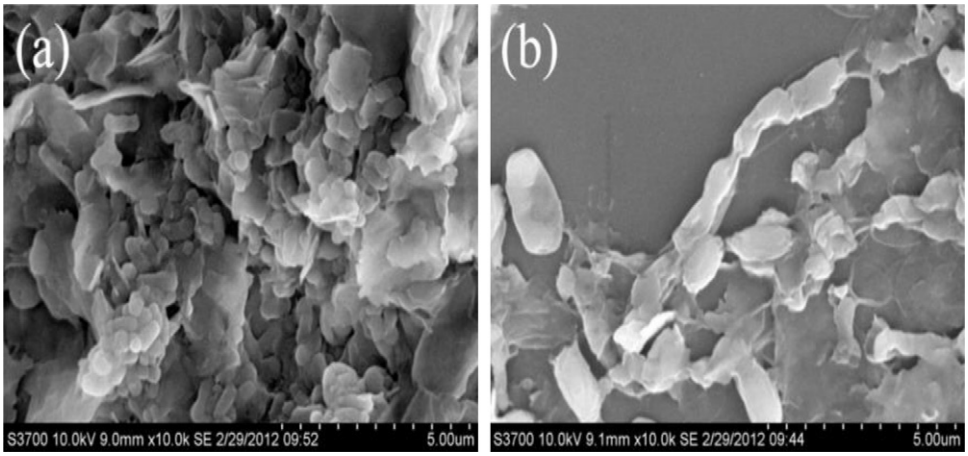

Fig. 6. SEM images of bacterial cells after the treatment with QCOR-4 nanocomposite: (a) *Pseudomonas aeruginosa* and (b) *Bacillus subtilis*.

3.4. Antimicrobial activity of QCOR nanocomposites

Table 1 lists the minimum inhibition concentration (MIC) of REC, QCMCO and QCOR nanocomposites against microorganisms. As shown in the table, pure rectorite has not antimicrobial activity, whereas QCMCO shows slight inhibitory effect on the growth of Gram-negative bacteria, Gram-positive bacteria and fungus. Compared to QCMCO, the MICs of QCOR nanocomposites were lower,

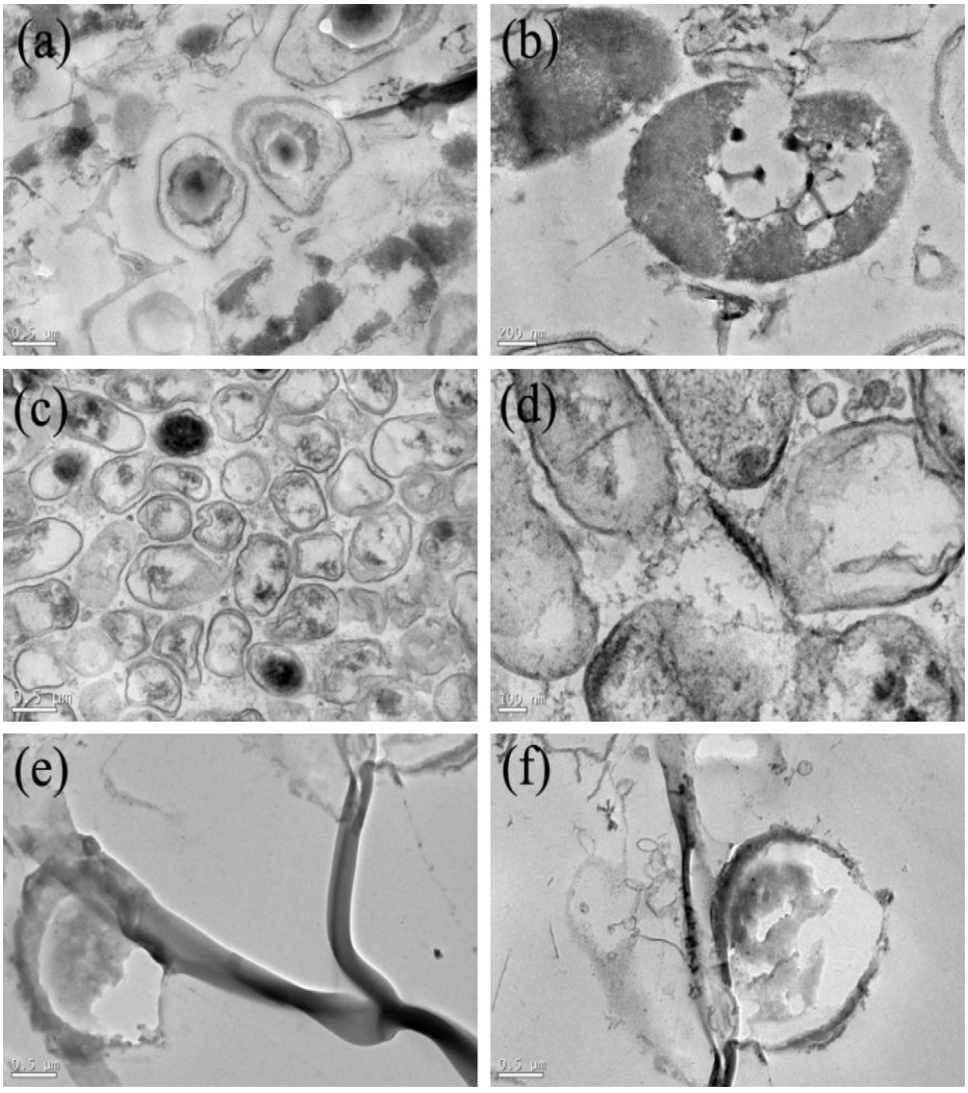

Fig. 7. TEM images of microorganisms cells after the treatment with QCOR-4 nanocomposite: (a, b) *Bacillus subtilis*; (c, d) *Pseudomonas aeruginosa*; and (e, f) *Aspergillus niger*.

indicating that the antimicrobial activity of QCOR nanocomposites were stronger than QCMCO, and increased with the QCMCO content. Moreover, the inhibitory property of QCOR nanocomposites for Gram-positive bacteria was better than that for Gram-negative bacteria and fungus.

Fig. 6 shows the SEM images of *P. aeruginosa* (a) and *B. subtilis* (b) which were treated by QCOR-4 nanocomposite, surface collapse and deformation of both bacteria can be observed. Fig. 7 gives the TEM internal slice images of *P. aeruginosa*, *B. subtilis* and *Aspergillus niger* which were also treated by QCOR-4 nanocomposite, it can see clearly that after the treatment with QCOR-4 nanocomposite, the shape of Gram-positive bacteria and Gram-negative bacteria turned to irregular, bacterial cell wall broke and the cell contents infiltrated, and thereby the cells lost activity. In addition, fungus *Aspergillus niger* spore split after the treatment with QCOR-4 nanocomposite, and its normal physiological activity was also inhibited.

It was reported that original REC possessed certain adsorption capacity, it can adsorb and fix bacteria (as shown in Fig. 7d) (X. Wang et al., 2009, 2006; X.Y. Wang et al., 2009), zeta potential results indicate that QCMCO is a positively charged polyelectrolyte, so it could interact with negatively charged bacteria at the cell surface, change the bacterial cell membrane permeability, restrain the growth of the cell and even cause the death of the cell (Kong et al., 2010). Since chitosan-based layered silicate nanocomposite can combine both advantages of polymer and layered silicate, antimicrobial property of QCOR nanocomposites improved compared with QCMCO and REC. It can be inferred that firstly REC adsorbed and fix bacteria, and then QCMCO exerted the antimicrobial activity (X. Wang et al., 2006).

Moreover, it can find that the antimicrobial activity of QCOR nanocomposites enhanced with the increase of QCMCO amount. On the one hand, high amount of QCMCO could enhance the positive zeta potential value of QCOR nanocomposites, which benefited the interaction with negative bacteria surface; on the other hand, the increase of QCMCO also provided more quaternary ammonium groups which could react with the bacteria.

Furthermore, it can find from Table 1 that the inhibitory activity against Gram-negative bacteria and fungus for QCMCO and QCOR nanocomposites was not as good as that against Gram-positive bacteria. This may be related to the cell structure of the bacteria. Gram-positive bacteria have thick cell wall and no outer membrane, whereas Gram-negative bacteria have thin cell wall and the outer membrane, so it can effectively prevent the invasion of foreign objects, but compared with bacterium, fungus is the heterotrophic organism with eukaryotic and cell wall and is hard to suppress, therefore, the inhibition activity of QCMCO against the microorganisms was different (Dutta et al., 2012), and the adsorption effect of REC for these three microorganisms may be different (X. Wang et al., 2006).

4. Conclusions

QCOR nanocomposites with maximum interlayer distance of 2.68 nm were successfully synthesized under the condition of microwave radiation in 70 min, QCMCO and REC connected through hydrogen bonds and electrostatic interactions, which resulted in the change of crystallization behavior of QCOR nanocomposites and the improved residual weight of QCOR nanocomposites compared with QCMCO, but REC has little impact on the maximum thermal degradation temperature of QCOR nanocomposite. Furthermore, compared with QCMCO, QCOR nanocomposites showed stronger antibacterial activity in the presence of REC, which was positive to the content of QCMCO, what's more, the inhibition effect on Gram-positive bacteria was better than that of Gram-negative bacteria and fungus.

Acknowledgements

This work was financially supported by the National Natural Science Foundation of China (No. 30972323), Science & Technology Project of Guangzhou City in China (No. 2012J2200018), the Fundamental Research Funds for the Central Universities, SCUT (No. 2012ZZ0080) and Science & Technology Project of Guangdong Province in China (No. 2011B050400015).

References

Aranaz, I., Harris, R., & Heras, A. (2010). Chitosan amphiphilic derivatives. Chemistry and applications. *Current Organic Chemistry*, *14*(3), 308–330.
Cheng, K.-C., Yu, C.-B., Guo, W., Wang, S.-F., Chuang, T.-H., & Lin, Y.-H. (2012). Thermal properties and flammability of polylactide nanocomposites with aluminum trihydrate and organoclay. *Carbohydrate Polymers*, *87*(2), 1119–1123.
Deng, H., Lin, P., Xin, S., Huang, R., Li, W., Du, Y., et al. (2012). Quaternized chitosan-layered silicate intercalated composites based nanofibrous mats and their antibacterial activity. *Carbohydrate Polymers*, *89*(2), 307–313.
De Paiva, L. B., Morales, A. R., & Valenzuela Diaz, F. R. (2008). Organoclays: Properties, preparation and applications. *Applied Clay Science*, *42*(1–2), 8–24.
Dutta, J., Tripathi, S., & Dutta, P. K. (2012). Progress in antimicrobial activities of chitin, chitosan and its oligosaccharides: A systematic study needs for food applications. *Food Science and Technology International*, *18*(1), 3–34.
El-Sherif, H., & El-Masry, M. (2011). Superabsorbent nanocomposite hydrogels based on intercalation of chitosan into activated bentonite. *Polymer Bulletin*, *66*(6), 721–734.
Gedye, R., Smith, F., & Westaway, H. A. (1986). The use of microwave ovens for rapid organic synthsis. *Tetrahedron Letters*, *27*(3), 279–282.
Kabiri, K., Mirzadeh, H., & Zohuriaan-Mehr, M. J. (2007). Highly rapid preparation of a bio-modified nanoclay with chitosan. *Iranian Polymer Journal*, *16*(3), 147–151.
Karim, M. R., Lee, H. W., Kim, R., Ji, B. C., Cho, J. W., Son, T. W., et al. (2009). Preparation and characterization of electrospun pullulan/montmorillonite nanofiber mats in aqueous solution. *Carbohydrate Polymers*, *78*(2), 336–342.
Kong, M., Chen, X. G., Xing, K., & Park, H. J. (2010). Antimicrobial properties of chitosan and mode of action: A state of the art review. *International Journal of Food Microbiology*, *144*(1), 51–63.
Liu, B., Wang, X. Y., Yang, B., & Sun, R. C. (2011). Rapid modification of montmorillonite with novel cationic Gemini surfactants and its adsorption for methyl orange. *Materials Chemistry and Physics*, *130*(3), 1220–1226.
Liu, B., Wang, X. Y., Yang, B., Wang, X. H., & Sun, R. C. (2011). Microwave irradiation-assisted synthesis and flocculation behavior of quaternized chitosan/organo-montmorillonite nanocomposite. *Current Nanoscience*, *7*(6), 1034–1041.
Liu, B., Wang, X. Y., Li, X. Y., Zeng, X. J., Sun, R. C., & Kennedy, J. F. (2012). Rapid exfoliation of rectorite in quaternized carboxymethyl chitosan. *Carbohydrate Polymers*, *90*, 1826–1830.
Liu, B., Wang, X. Y., Yang, B., & Sun, R. C. (2012). Microwave-assisted synthesis of quaternized carboxymethyl chitosan in aqueous solution and its thermal behavior. *Journal of Macromolecular Science Part A – Pure and Applied Chemistry*, *49*(3), 227–234.
Luo, J. W., Wang, X. Y., Xia, B., & Wu, J. (2010). Preparation and characterization of quaternized chitosan under microwave irradiation. *Journal of Macromolecular Science Part A – Pure and Applied Chemistry*, *47*(9), 952–956.
Mecwan, M. M., Rapalo, G. E., Mishra, S. R., Haggard, W. O., & Bumgardner, J. D. (2011). Effect of molecular weight of chitosan degraded by microwave irradiation on lyophilized scaffold for bone tissue engineering applications. *Journal of Biomedical Materials Research Part A*, *97A*(1), 66–73.
Ojijo, V., Malwela, T., Ray, S. S., & Sadiku, R. (2012). Unique isothermal crystallization phenomenon in the ternary blends of biopolymers polylactide and poly (butylene succinate)-co-adipate and nano-clay. *Polymer*, *53*(2), 505–518.
Sun, L. P., Du, Y. M., Fan, L. H., Chen, X., & Yang, J. H. (2006). Preparation, characterization and antimicrobial activity of quaternized carboxymethyl chitosan and application as pulp-cap. *Polymer*, *47*(6), 1796–1804.
Tishchenko, G., Simunek, J., Brus, J., Netopilik, M., Pekarek, M., Walterova, Z., et al. (2011). Low-molecular-weight chitosans: Preparation and characterization. *Carbohydrate Polymers*, *86*(2), 1077–1081.
Vinsova, J., & Vavrikova, E. (2011). Chitosan derivatives with antimicrobial, antitumour and antioxidant activities: A review. *Current Pharmaceutical Design*, *17*(32), 3596–3607.
Wang, Q., Hu, X., Du, Y., & Kennedy, J. F. (2010). Alginate/starch blend fibers and their properties for drug controlled release. *Carbohydrate Polymers*, *82*(3), 842–847.
Wang, Q., Zhang, N., Hu, X., Yang, J., & Du, Y. (2008). Chitosan/polyethylene glycol blend fibers and their properties for drug controlled release. *Journal of Biomedical Materials Research Part A*, *85A*(4), 881–887.
Wang, Q., Zhang, N., Hu, X., Yang, J., & Du, Y. (2007). Alginate/polyethylene glycol blend fibers and their properties for drug controlled release. *Journal of Biomedical Materials Research Part A*, *82A*(1), 122–128.

Wang, X., Du, Y., Luo, J., Lin, B., & Kennedy, J. F. (2007). Chitosan/organic rectorite nanocomposite films: Structure, characteristic and drug delivery behaviour. *Carbohydrate Polymers*, *69*(1), 41–49.

Wang, X., Du, Y., Yang, H., Wang, X., Shi, X., & Hu, Y. (2006). Preparation, characterization and antimicrobial activity of chitosan/layered silicate nanocomposites. *Polymer*, *47*(19), 6738–6744.

Wang, X., Du, Y., Luo, J., Yang, J., Wang, W., & Kennedy, J. F. (2009). A novel biopolymer/rectorite nanocomposite with antimicrobial activity. *Carbohydrate Polymers*, *77*(3), 449–456.

Wang, X. Y., Du, Y. M., Sun, R. C., & Lin, L. (2009). Chitosan-based layered silicate nanocomposites. *Progress in Chemistry*, *21*(7–8), 1507–1514.

Wang, X. Y., Liu, B., Ren, J. L., Liu, C. F., Wang, X. H., Wu, J., et al. (2010). Preparation and characterization of new quaternized carboxymethyl chitosan/rectorite nanocomposite. *Composites Science and Technology*, *70*(7), 1161–1167.

Wang, X. Y., Liu, B., Tang, Y. F., Su, H. J., Han, Y., & Sun, R. C. (2012). New progress on rectorite/polymer nanocomposites. *Journal of Inorganic Materials*, *27*(2), 113–121.

Xia, W., Liu, P., Zhang, J., & Chen, J. (2011). Biological activities of chitosan and chitooligosaccharides. *Food Hydrocolloids*, *25*(2), 170–179.

Zhou, Y., Chen, H. L., Yao, J., He, M. Y., Si, Y., Feng, L. A., et al. (2010). Influence of clay minerals on the Bacillus halophilus Y38 activity under anaerobic condition. *Applied Clay Science*, *50*(4), 533–537.